Liquid Chromatography–Mass Spectrometry with Collision-Induced Dissociation of Conjugated Metabolites of Benzo[*a*]pyrene

Y. Yang,* W. J. Griffiths, and J. Sjövall

Department of Medical Biochemistry and Biophysics, Karolinska Institute, Stockholm, Sweden

J.-Å. Gustafsson and J. Rafter

Department of Medical Nutrition, Karolinska Institute, Huddinge University Hospital, NOVUM, Stockholm, Sweden

Benzo[*a*]pyrene (BP) metabolites conjugated with glutathione, cysteine-glycine, cysteine, *N*-acetylcysteine, and sulfuric and glucuronic acids have been studied by microcolumn liquid chromatography–electrospray mass spectrometry with collision-induced dissociation (CID) on a hybrid double focusing magnetic sector–orthogonal time-of-flight tandem mass spectrometer equipped with a focal plane array detector. Negative-ion electrospray mass spectra of the conjugated BP metabolites showed strong $[M - H]^-$ ions. When the array detector was used, spectra were obtained from femtomoles of sample infused at mass resolutions of 5000 (full width at half maximum). Cone voltage fragmentation spectra show $[M - H]^-$ ions and fragment ions indicative of the BP moiety and/or the conjugating group. Linked scan CID spectra at constant B/E were found to contain structurally informative product ions from infusion of as little as 1 pmol of sample. CID spectra were also recorded by using the double focusing sectors for precursor ion selection and the orthogonal time-of-flight analyzer for product ion mass separation. The method was applied to the analysis of conjugated BP metabolites in the urine of germ-free rats given a single intraperitoneal dose of BP. © *1997 American Society for Mass Spectrometry (J Am Soc Mass Spectrom 1997, 8, 50–61)*

Polycyclic aromatic hydrocarbons (PAH) are widely distributed in the environment and suspected to be a significant health risk to humans [1]. Benzo[*a*]pyrene (BP) (Structure **1**), one of the most studied PAHs, undergoes extensive metabolism to a number of compounds, including some highly reactive electrophiles that can form covalent bonds with macromolecules, including DNA [2]. Some of these reactive intermediates, for example, PB *r*-7-*t*-8-dihydrodiol-*t*-9,10-epoxide (BPDE) (Structure **2**), in particular the (+)-enantiomer, have been shown to be potent mutagens and carcinogens in various experimental systems [3]. Glucuronidation and sulfation are two major reaction pathways to convert highly electrophilic intermediates of BP metabolism into water soluble substances that can be readily excreted [4]. Glutathione conjugation of BP with subsequent formation of mercapturic acid pathway metabolites represents another detoxification pathway which is important in the liver [5]. The importance of the mercapturic acid pathway in the in vivo metabolism of BP has been reported [6]. Characterization of BP metabolites has been performed predominantly in connection with in vitro experiments. In vivo studies have been severely hampered by analytical problems caused by the variety, polarity, and low concentrations of BP metabolites in biological extracts.

In an earlier publication from our laboratory, a group fractionation procedure was reported as the first step in the analysis of BP metabolite mixtures in rate excreta [7, 8]. This separates neutral or weakly acidic unconjugated BP metabolites and different classes of intact conjugates of BP metabolites. The pattern of BP metabolites observed in vivo was far more complex than what can be deduced from previous studies [9, 10]. About 18% of the BP derivatives in urine were neutral or weakly acidic compounds. Among them, a number of novel metabolites were detected by using high-performance liquid chromatography (HPLC) and gas chromatography–mass spectrometry (GC/MS) [11]. Attempts were made to analyze the conjugated

Address reprint requests to Dr. W. J. Griffiths, Department of Medical Biochemistry and Biophysics, Karolinska Institute, S-171 77 Stockholm, Sweden.

*Also affiliated with Department of Medical Nutrition, Karolinska Institute, Huddinge University Hospital, Stockholm, Sweden.

1044-0305/97/$17.00
PII S1044-0305(96)00136-5

Received March 27, 1996
Revised August 7, 1996
Accepted August 16, 1996

BP metabolites that predominate in rate excreta (about 80% of BP derivatives) by using static and continuous-flow fast-atom bombardment mass spectrometry (CF-FAB/MS). Because of the complexity of the mixture, the instability of some metabolites during the purification process, and an insufficient yield of ions by these methods, the analysis of BP conjugates in biological fluids has been problematic [12–14].

Electrospray (ES) [15] is an alternative soft ionization technique that has been widely used in the characterization of biological substances and perhaps is more appropriate for the analysis of conjugated BP metabolites. When combined with the use of a focal plane array detector in a magnetic sector mass spectrometer, a great increase in sensitivity may be expected.

HPLC has been extensively used in the analysis of metabolites of xenobiotics, particularly their conjugated forms. Trace analysis with capillary column HPLC can be achieved with high column efficiency, low sample consumption, and microliter flow rates compatible with direct connection to ES or continuous-flow fast-atom bombardment (CF-FAB) ion sources. Liquid chromatography–mass spectrometry (LC/MS) is potentially the most suitable method for the analysis of conjugated metabolites of xenobiotics and endogenous substances in biological material. In our laboratory, capillary liquid chromatography–fast-atom bombardment mass spectrometry (LC-FAB/MS) and liquid chromatography–electrospray mass spectrometry (LC-ES/MS) have been used to analyze metabolites of arachidonic acid [16] and bile acids in human urine (Yang, Y.; Griffith, W. J.; Nazer, H.; Sjövall, J., unpublished).

Since CF-FAB/MS did not provide the required sensitivity in analyses of conjugated BP metabolites [12], in the present study we have investigated the possibility that this could be achieved by ES ionization alone and in combination with capillary column HPLC. The mass spectrometer used was a hybrid magnetic sector (EBE) orthogonal time-of-flight (TOF) instrument equipped with a focal plane array detector (FPD) positioned after the magnetic sector [17, 18].

Studies were performed to determine sensitivities and optimum conditions for the identification of urinary metabolites of BP (Structures **3–14**) by using electrospray mass spectrometry (ES/MS) with collision-induced dissociation (CID). The detection limits for a series of conjugated BP metabolites have been determined with both point and focal plane array detectors. Cone voltage collision-induced dissociation (CVCID) spectra, high translational energy CID B/E linked scan spectra, and 400-eV orthogonal acceleration time-of-flight (OATOF) CID spectra have been recorded and compared. Capillary column HPLC-ES-CID has also been applied to the analysis of conjugated BP metabolites in the urine of rats after a single dose of BP. However, the thorough characterization of in vivo metabolites of BP in both urine and faces of rats given BP will be published in separate articles.

Experimental

Chemicals

Analytical grade solvents were redistilled prior to use. Water was distilled and deionized in a Milli-Q water system (Millipore, Molsheim, France). Racemic BPDE, sodium salts of BP-3-ol-β-D-glucuronide (BP-3-GlcA), BP-9-ol-β-D-glucuronide (BP-9-GlcA), and BP-9-ol-sulfate (BP-9-SO_4) were obtained from the National Cancer Institute, Chemical Carcinogens Repositories (National Institute of Health, Bethesda, MD). The glutathione (GSH), cysteinyl-glycine (CysGly), cysteine (Cys), and *N*-acetylcysteine (NAcCys) conjugates of BPDE (BPDE-GSH, BPDE-CysGly, BPDE-Cys, and BPDE-NAcCys) were synthesized as described previously [12]. NAcCys, Cys, CysGly, and GSH conjugates of BPDE each eluted, as expected, as two peaks in the HPLC chromatograms due to the presence of diastereoisomers. These isomers were not separated from the mass spectrometric analysis.

Animal Treatment

Germ-free rats were dosed intraperitoneally with a mixture of BP (Sigma, St. Louis, MO) and [7,10-^{14}C] labeled BP (Amersham International, England; 16.7 μg/g body weight) and urine was collected as described previously [11].

Chromatographic System

The capillary column (0.25 mm i.d. × 500 mm, packed with 5-μm Chromasil C_{18} (Hichrom, Berkshire, UK) as described by Alborn and Stenhagen [19]) was connected to a transfer capillary of fused-silica tubing (0.05 mm × 1 m). About 10 mm of the polyimide coating of this capillary was removed to provide a flow cell for UV detection by using an ISCO detector (model CV4, Lincoln, NE) at a wavelength of 254 nm. A flow rate of 5 μL/min was generated with a Carlo Erba syringe pump (Fisons Instrument, UK) in the pressure control mode. The mobile phase consisted of 60% methanol/water. A Valco (Houston, TX) C6 injection valve with an external loop (20 μL) was used for injection of the sample in 2–10 μL of mobile phase containing a higher concentration of water than that used in the chromatography to concentrate the analytes at the top of the column.

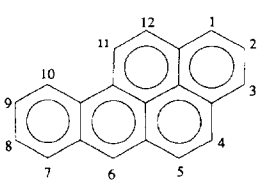

BP (1)

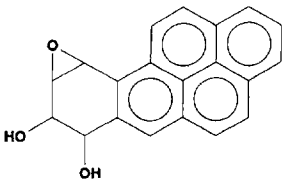

BPDE (2)

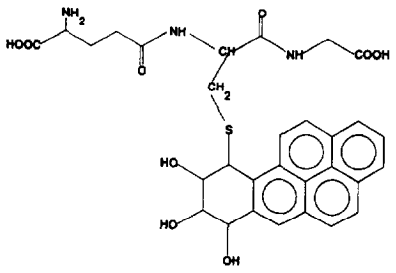

BPDE-10-GSH (3)

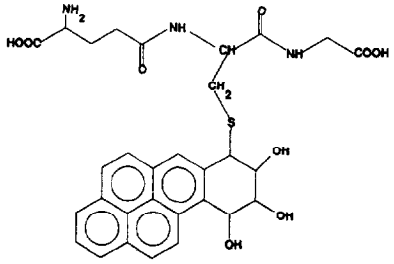

BPDE-7-GSH (4)

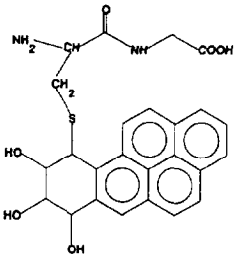

BPDE-10-CysGly (5)

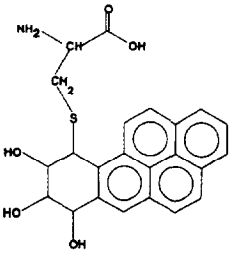

BPDE-10-Cys (6)

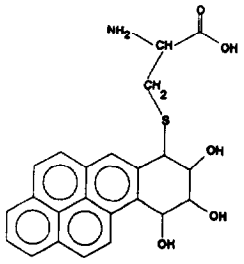

BPDE-7-Cys (7)

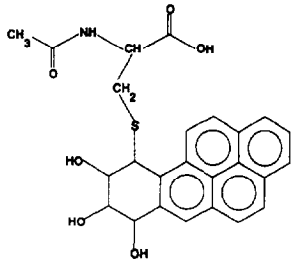

BPDE-10-NAcCys (8)

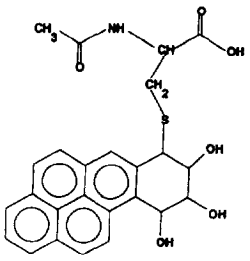

BPDE-7-NAcCys (9)

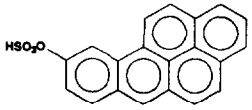

BP-9-SO_4 (10)

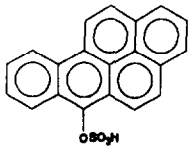

BP-6-SO_4 (11)

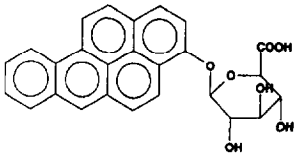

BP-3-GlcA (12)

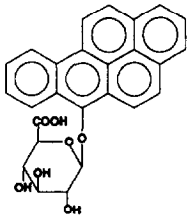

BP-6-GlcA (13)

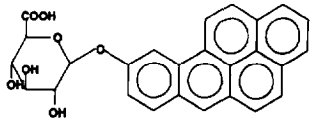

BP-9-GlcA (14)

Mass Spectrometry

Negative-ion ES mass spectra were recorded on a VG (formerly VG Analytical, now Micromass, Manchester, UK) AutoSpec-TOFFPD hybrid mass spectrometer (described fully in refs 17 and 18). The sample solutions of HPLC effluents were transferred directly into the electrospray source. An accelerating voltage of −4 kV was selected and nitrogen was used as the nebulizer and bath gas with flow rates of 15 and 250 L/h, respectively. The bath gas was heated to 80 °C.

To record spectra by using the point and array detectors, the source was tuned to give a maximum $[M - H]^-$ ion current at a resolution of 1000 (5% valley) and 5000 (full width at half maximum), respectively.

High translational energy CID spectra were generated by using helium as the collision gas in the first field-free region gas cell at a pressure that gave a reduction of 50% in $[M - H]^-$ ion intensity. The laboratory frame collision energy was 4000 eV. Product ion, constant B/E linked scan spectra were recorded by using the FPD set at a mass ratio setting of 1.05 : 1 and with exposure times of 1–2 seconds per exposure.

To record the CID spectra on the TOF analyzer, the EBE section of the AutoSpec mass spectrometer was employed as mass spectrometer 1 (MS1) and $[M - H]^-$ ions were selected and focused into the collision cell located just after the collector slit. MS1 was operated at a resolution of approximately 1500 (5% valley). The cell was floated to −3.6 kV, thereby giving a collision energy of 400 eV in the laboratory frame. Xenon was used as the collision gas.

Results and Discussion

Detection Limits on the Point and Array Detectors with Constant Infusion of Conjugated BP Metabolites

As previous mass spectrometric studies of conjugated BP-metabolites were ineffective due to insufficient instrumental sensitivity, initial experiments were performed to determine the optimum conditions and limits of sensitivity for analysis of such compounds. The ES solvent was selected to give maximum intensity of the $[M - H]^-$ ion. In most cases, this was obtained when samples were dissolved in methanol/water (1 : 1 by volume). However, the addition of 1% ammonia enhanced the signal 2–3 times for the amphoteric, that is, Cys and CysGly, conjugates. When the solvent system was acetonitrile/water (1 : 1 by volume) or 50% methanol buffered with 30-mM ammonium acetate (pH 7.2); used to obtain the best chromatographic separation) the $[M - H]^-$ ion intensity was 50% of that obtained with a ~ 50% methanol solvent system.

The detection limits were determined at a constant infusion flow rate of 5 μL/min methanol/H_2O (1 : 1 by volume) solvent. Lowering the flow rate from 5 to 2 μL/min had no noticeable effect on ion current when the sampling cone and counter electrode were freshly cleaned and the needle was carefully positioned. However, there was a reduction in signal stability at low flow rates as the counter electrode and cone steadily became dirtier. Some instability of the ion current also resulted when 30% methanol was used as the solvent.

Full mass spectra were recorded by using both the point and array detectors. Table 1 summarizes the results obtained. Detection limits are quoted for a minimum of 10 : 1 signal-to-noise ratio and are for the amount of infused sample. A full mass spectrum was recorded at the point detector in approximately 15 s (1 min on the FPD) during which time 1.25 μL (5 μL on FPD) of sample solution was sprayed into the instrument. For the GSH conjugate, infusion of 1.4 fmol of sample was sufficient to give a full mass spectrum by using the FPD, while approximately 100 times more sample was required to obtain a similar signal-to-noise (S/N) ratio with the point detector. From Table 1 it can be seen that by using the FPD rather than the point detector, the detection limits for all the BP metabolites studied were improved by an order of magnitude. By selecting a narrow mass range where the $[M - H]^-$ ion appears, the amount of sample infused to give a spectrum in which the $[M - H]^-$ ion dominates can be reduced by another factor of 5–10. Although the amount of sample infused to record a spectrum is a somewhat artificial figure, it is relevant as it indicates a lower limit of sample which theoretically can be analyzed on the instrument.

In a previous article we reported on the analysis of conjugated BP metabolites by static and continuous-flow fast-atom bombardment mass spectrometry (FAB/MS) on a VG 70-250 instrument equipped with an electron multiplier point detector [12]. With static FAB/MS, 4 nmol of material gave S/N ratios of 5 : 1

Table 1. Detection of BP metabolite conjugates on the point and array detectors with constant infusion of sample: the recording of full mass spectra at the point detector took approximately 15 s (1 min at the FPD) during which time 1.25 μL (5 μL on the FPD) was sprayed into the instrument

BP metabolite conjugate	Sample infused per scan	
	Point	Array
BPDE-GSH	50 pg 140 fmol	0.5 pg 1.4 fmol
BPDE-NAcCys	50 pg 180 fmol	5 pg 18 fmol
BPDE-CysGly	500 pg 1.7 pmol	5 pg 17 fmol
BPDE-Cys	5 ng 20 pmol	50 pg 200 fmol
BPDE-Cys (with 1% NH_3)	2 ng 8 pmol	
BP-Sulfate	50 pg 240 fmol	5 pg 24 fmol
BP-Glucuronide	500 pg 2 pmol	50 pg 200 fmol

for the cysteine conjugates and 20:1 for the glutathione conjugates. CF-FAB enhanced the sensitivity over static FAB by a factor of 4. With ES as the ionization method, the detection limits by using the point detector were 50 times lower for the cysteine conjugates and over 100 times lower for other conjugated BP metabolites. Further gains in sensitivity were obtained by recording ES spectra on the FPD. As a consequence of the chemical noise associated with CF-FAB, similar gains in sensitivity would not be obtained by using the FPD in association with this form of ionization. It should also be mentioned that although $[M - H]^-$ ions were dominated in both FAB and ES spectra, FAB/MS gave intense fragment ions indicative of the BP moiety and conjugating group, while there was little fragmentation observed in conventional ES spectra.

Capillary Column–High-Performance Liquid Chromatography–Electrospray Mass Spectrometry of a Mixture of Conjugated BP Metabolites

The four mercapturic acid pathway BP metabolites—GSH, CysGly, Cys, and NAcCys conjugates of BP-7,8-dihydrodiol-9,10-epoxide—were used in the present study to demonstrate the effectiveness of capillary column-HPLC-ES/MS (high-performance liquid chromatography–electrospray mass spectrometry) for analysis of conjugated BP metabolites. Gradient elution with methanol/water containing 30-mM ammonium acetate buffer (pH 7.2) was used at a flow rate of 4 μL/min. Detection limits were also determined by using the LC inlet system for the amount of sample injected. Detection limits were at picomole levels for full mass spectra recorded on the point detector and were not greatly dissimilar from those determined by continuous infusion.

4000-eV, 400-eV, and Cone Voltage Collision-Induced Dissociation of BP Metabolite Conjugates

As outlined in the Experimental section CID spectra were recorded at high translational energy (4000 eV) by using He as the collision gas. These were linked scans at constant B/E and recorded on the FPD. CID spectra were also recorded by using the OATOF analyzer. In such cases Xe was the collision gas employed and the laboratory frame collision energy was 400 eV. By using Xe as the collision gas, high center of mass collision energies are attained even at intermediate laboratory frame collision energies.

Cone voltage spectra are recorded when the potential difference between the sampling cone and the skimmer is approximately 300 V. If the sample is pure, the mass spectrum recorded will be a CID spectrum of the sample. As CVCID occurs without mass selection of the precursor ion, the presence of impurities will also lead to peaks in the spectrum indistinguishable from CVCID fragments.

The CID spectra presented were recorded with continuous infusion of sample, unless otherwise stated.

Fragmentation Nomenclature

For a molecule M, the deprotonated molecule $[M - H]^-$ is represented as 'M, where the prime to the left of the capital letter indicates that the ion is deficient in one H compared to the molecular ion. Similarly a double prime to the left of the capital letter representing a fragmentation process indicates that fragmentation proceeds with the resulting fragment ion, for example, $''X_1$ is deficient in two hydrogens as compared with a fragment ion formed by a homolytic fragmentation at the same point in the molecular ion M^-. Primes to the right indicate the addition of H to the fragment.

The benzo[*a*]pyrene moiety is represented by BP and the benzo[*a*]pyrene tetrahydrotriol moiety by A (adducting group).

Peptide fragmentation will be described by using the nomenclature of Roepstorff and Fohlman [20]. The notation to describe the H transfer upon fragmentation will be similar to that proposed by Roepstorff and Fohlman.

Collision-Induced Dissociation of BPDE-10-GSH and BPDE-7-GSH

CID spectra were recorded for BPDE-10-GSH and BPDE-7-GSH. Shown in Figure 1a and described in Table 2 is the 400-eV CID spectrum of the $[M - H]^-$ of BPDE-10-GSH recorded on the OATOF. The resolving properties of the EBE sectors of MS1 allow the selection of the monoisotopic (^{12}C) precursor ion. Unit mass resolution is achieved on the product ions. A weak fragment ion appears at m/z 563 but almost no other fragment ions are observed above mass m/z 336. Below m/z 336, peaks appear at m/z 335 and 334, probably corresponding to S-containing polycyclic hydrocarbon ions AS and 'AS formed by fragmentation of the C–S bond of cysteine (Scheme I), without (AS) and with ('AS) elimination of an H from the ring system. Intense fragment ions observed at m/z 305 ($'\gamma$) correspond to distonic glutathionate radical anions probably formed by a charge-remote fragmentation mechanism [21]. Fragment ions corresponding to the ring system at m/z 303 (A) are not observed. This is in contrast to the positive-ion CID of BPDE-DNA and BPDE-peptide adducts [22–24]. The fragment ion at m/z 272 is significant and probably corresponds to fragmentation of the C–S bond in cysteine with charge residing on the peptide ($''\beta$). The next intense peak appears at m/z 171 ($'X_2\beta$). This corresponds to a peptide ion formed by fragmentation at the C–S bond of cysteine and the bond between the carbonyl and

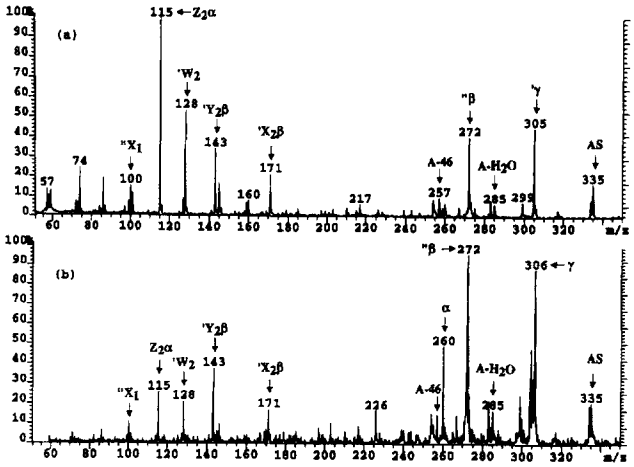

Figure 1. CID spectra of the $[M - H]^-$ ion of BPDE-10-GSH (m/z 608). (**a**) 400-eV collisions with Xe; spectrum recorded with the OATOF. (**b**) 4000-eV collisions with He; B/E linked scans recorded with the array detector.

CH_2 groups of glutamic acid. A further intense peak appears 28 u below this at m/z 143 ($'Y_2\beta$), as a consequence of the further loss of CO. Peptide fragmentation continues to give peaks at m/z 128 ($'W_2$) and m/z 115 ($Z_2\alpha$). Low mass fragment ions appear at m/z 100, 86, 74, and 57, characteristic of the glutathione fragments $C_3H_2O_3N$ ($"X_1$) or $C_4H_6O_2N$, $C_3H_4O_2N$, $C_2H_4O_2N$, and C_2HO_2, respectively.

The 4000-eV CID spectrum of BPDE-10-GSH (Figure 1b) is similar to that recorded at 400 eV. There are however some significant differences. In the 4000-eV collision, intense M-46 and M-76 fragmentations (see Other Ions in the CID Spectra in Table 2) occur, and a triplet appears at m/z 304 ($"\gamma$), 305 ($'\gamma$), and 306 (γ). Each ion is probably formed by fragmentation of the C–S bond with charged residing on the peptide fragment. Fragmentation of this bond has been found to give ions at m/z 305 in the CID of the glutathione conjugate leukotriene (LTC_4) [21] and 306 in the CID of xenobiotic glutathione conjugates [25]. The fragment ion at m/z 260 is considerably more intense in the 4000-eV spectrum than in the 400 eV and probably corresponds to the fragment α (Scheme I). The peptide fragmentations in both spectra are similar; however, fewer low mass peptide fragment ions are observed at 4000 eV than at 400 eV.

The CVCID spectrum of BPDE-10-GSH was also recorded and is described in Table 2. There are many similar features between this, and the 400- and 4000-eV CID spectra. The most noticeable difference in the CVCID spectrum as opposed to the 4000- and 400-eV CID spectra is the almost complete absence of peptide fragments in the CVCID spectrum. The only significant peptide fragmentation is at $"\beta$. Care must be taken when drawing conclusions from CVCID spectra as contaminant ions may be present that introduce confusion to the interpretation of the spectrum.

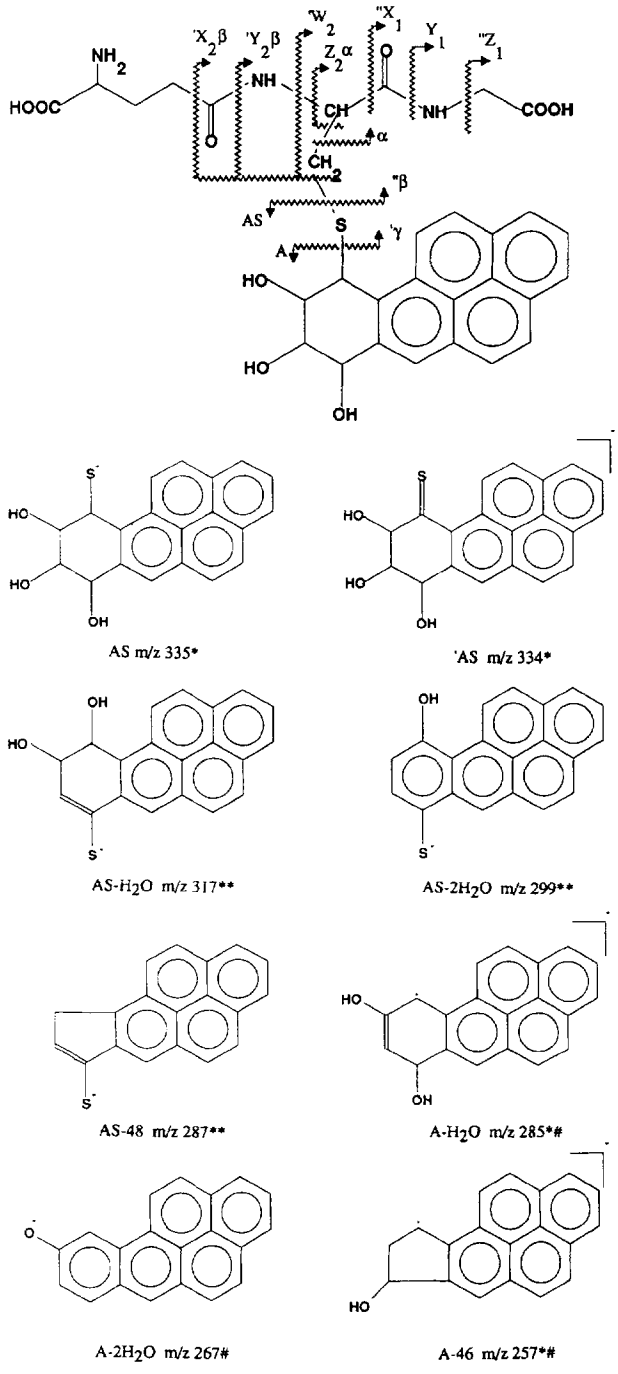

Scheme I. Fragmentation of BPDE-GSH. The peptide has been drawn conjugated to the BP-triol at position 10. Drawn for the 10-isomer (*), the 7-isomer (**), or the positional isomer (#).

The 4000- and 400-eV CID spectra of the BPDE-7-GSH are shown in Figure 2. Although they are similar to those of the BPDE-10-GSH, there are reproducible differences that allow isomer differentiation. The most striking difference in the CID spectra of the two isomers is the presence of a much stronger fragment ion at m/z 299 (AS-$2H_2O$) from BPDE-7-GSH than from BP-10-GSH. This a characteristic of the CID of the BPDE-7-cysteinyl conjugates studied (Table 2), as are the enhanced intensities of fragment ions at m/z 317

Table 2. Mass-to-charge ratio of fragment ions formed in the CID of deprotonated molecules of BPDE conjugates[a]

M − H	10-GSH 608				7-GSH 608				10-CysGly 479				10-NAcCys 464			
AS	335	(14)[c]	(23)[d]	(74)[e]	335	(21)	(16)	(14)	335	(36)	(100)	(60)	335	(100)	(100)	(44)
'AS	334	(—)	(18)	(—)	334	(11)	(18)	(—)	334	(—)	(48)	(—)	334	(7)	(30)	(—)
AS-18	317	(3)	(6)	(20)	317	(8)	(11)	(5)	317	(5)	(18)	(22)	317	(11)	(10)	(17)
γ	306	(3)	(94)	(19)	306	(8)	(52)	(13)	177	(29)	(62)	(—)	162	(11)	(16)	(—)
'γ	305	(39)	(37)	(19)	305	(50)	(10)	(—)					161	(12)	(—)	(—)
AS-36	299	(7)	(28)	(100)	299	(37)	(100)	(48)	299	(16)	(70)	(100)	299	(5)	(6)	(100)
AS-48	287	(—)	(—)	(12)	287	(2)	(10)	(—)								
A-18	285	(5)	(15)	(13)	285	(—)	(—)	(—)	285	(28)	(55)	(51)	285	(6)	(6)	(—)
AS-52	283	(7)	(23)	(52)	283	(17)	(38)	(10)	283	(11)	(44)	(37)	283	(26)	(13)	(73)
A-28	275	(3)	(8)	(46)	275	(—)	(18)	(—)	275	(8)	(16)	(37)	275	(22)	(12)	(26)
"β	272	(30)	(100)	(93)	272	(60)	(90)	(100)	143	(100)	(64)	(—)	128	(5)	(3)	(—)
A-36	267	(5)	(15)	(55)	267	(5)	(11)	(10)	267	(14)	(30)	(72)	267	(—)	(3)	(38)
'α	259	(4)	(—)	(—)	259	(5)	(—)	(—)	130	(32)	(19)	(—)	115	(2)	(1)	(—)
A-46	257	(8)	(15)	(55)	257	(5)	(—)	(—)	257	(15)	(16)	(15)	257	(9)	(6)	(100)
A-64	239	(3)	(8)	(20)	239	(5)	(—)	(—)	239	(8)	(18)	(98)	239	(7)	(5)	(47)
$C_{17}H_{12}$	226	(4)	(17)	(—)	226	(5)	(4)	(—)					226	(—)	(3)	(—)
A-88					215	(—)	(8)	(—)	215	(—)	(61)	(62)	215	(2)	(3)	(2)
$'X_{1\gamma}$													146	(95)	(7)	(—)
$Z_2\alpha$	115	(100)	(25)	(2)	115	(100)	(10)	(—)	115	(95)	(22)	(—)				
γ − 60													102	(30)	(1)	(—)
$"X_1$	100	(14)	(6)	(—)	100	(21)	(13)	(—)	100	(26)	(18)	(—)				
$C_3H_4O_2N$	86	(19)	(3)	(—)	86	(18)	(—)	(—)	86	(10)	(—)	(—)				
$C_2H_4O_2N$	74	(24)	(—)	(—)	74	(38)	(2)	(—)	74	(41)	(4)	(—)	74	(47)	(—)	(—)
$C_2H_3O_2$	59	(12)	(2)	(—)	59	(6)	(—)	(—)	59	(46)	(—)	(—)	59	(51)	(—)	(—)
C_2HO_2	57	(13)	(—)	(—)	57	(16)	(—)	(—)	57	(31)	(2)	(—)	57	(7)	(—)	(—)

Other Ions in the CID Spectra

BPDE-10-GSH

m/z 563 M-46 (1) (57) (—); 533 M-76 (—) (25) (—); 304 γ (—) (48) (13); 260 α (5) (54) (—); 203 (—) (10) (—); 185 (4) (6) (—); 160 (7) (3) (—); 171 $'X_2$ β (20) (15) (6); 145 (16) (6) (—); 143 $'Y_2$ β (31) (39) (9); 128 $'W_2$ (49) (15) (—)

BPDE-7-GSH

m/z 563 M-46 (4) (20) (—); 533 M-76 (—) (18) (—); 304 γ (—) (31) (5); 260 α (5) (35) (—); 203 (—) (7) (—); 185 (7) (4) (—); 160 (8) (2) (—); 171 $'X_2$ β (27) (9) (—); 145 (18) (—) (—); 143 $'Y_2$ β (64) (40) (—); 128 $'W_2$ (78) (32) (—)

BPDE-10-CysGly

m/z 175 "γ (12) (49) (—); 243 A-60 (21) (40) (42); 160 (19) (6) (—)

BPDE-10-NAc-Cys

m/z 271 AS-64 (5) (6) (—); 247 AS-88 (7) (6) (66); 243 A-60 (5) (4) (—); 117 'γ-44 (36) (3) (—)

BPDE-7-NAcCys

m/z 345 M-120 (—)(11) (—); 269 A-34 (9) (—) (—); 255 A-48 (9) (—) (30); 117 'γ-44 (30) (—) (—)

BPDE-NAcCys (rat urine)

m/z 255 A-48 (10) (—)(—); 117 'γ-44 (12) (—) (—)

(continued)

Table 2. *(Continued)*

M − H	7-NAcCys 464				U-NAcCys[b] 464		10-Cys 422				7-Cys 422	
AS	335	(100)	(100)	(20)	335	(100)[c]	335	(100)	(100)	(55)	335	(64)[c]
'AS	334	(9)	(39)	(20)	334	(10)	334	(—)	(45)	(—)		
AS-18	317	(42)	(40)	(43)			317	(34)	(36)	(24)	317	(100)
γ	162	(10)	(28)	(7)	162	(10)	120	(27)	(12)	(—)	120	(17)
'γ	161	(12)	(4)	(—)								
AS-36	299	(12)	(28)	(100)	299	(20)	299	(26)	(18)	(76)	299	(35)
AS-48	287	(10)	(15)	(27)								
A-18							285	(28)	(25)	(48)		
AS-52	283	(28)	(21)	(80)	283	(18)	283	(33)	(23)	(76)	283	(14)
A-28					275	(10)	275	(32)	(16)	(24)		
"β	128	(17)	(7)	(—)	128	(16)						
A-36	267	(7)	(8)	(73)			267	(25)	(15)	(100)		
'α	115	(1)	(1)	(—)	115	(—)						
A-46							257	(18)	(12)	(69)		
A-64 $C_{17}H_{12}$	239	(10)	(11)	(57)	239	(—)	239	(32)	(6)	(100)		
A-88	215	(4)	(10)	(—)	215	(—)	215	(—)	(12)	(45)	215	(31)
$'X_{1\gamma}$ $Z_2\alpha$	146	(94)	(7)	(—)	146	(61)						
γ − 60	102	(20)	(—)	(—)	102	(11)						
$"X_1$ $C_3H_4O_2N$												
$C_2H_4O_2N$	74	(47)	(—)	(—)	74	(34)	(8)	(—)	74	(21)		
$C_2H_3O_2$ C_2HO_2	59	(17)	(4)	(—)	59	(13)	59	(80)	(3)	(—)		

[a]Relative intensities are shown in parentheses. Peptide fragmentations are described in Schemes I and III.
[b]BPDE-NAcCys in rat urine.
[c]In the 400-eV CID spectra.
[d]In the 4000-eV CID spectra.
[e]In the CVCID spectra.

(AS-H_2O) and 287 (AS-48) and the reduced intensity of ions at m/z 285 (A-H_2O) and 257 (A-46). Interestingly the fragment ions AS-2H_2O, AS-H_2O, and AS-48 are all sulfur-containing ions, while A-H_2O and A-46 are not. The two BPDE-GSH isomers can thus be differentiated from their 4000- or 400-eV CID spectra.

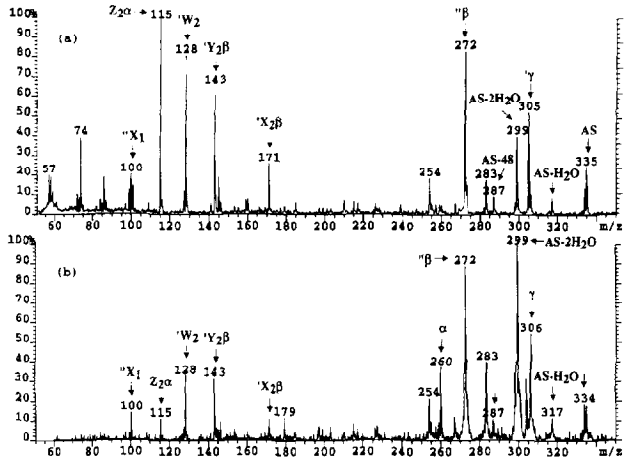

Figure 2. CID spectra of the $[M - H]^-$ ion of BPDE-7-GSH (m/z 608). (**a**) 400-eV collisions with Xe; spectrum recorded with the OATOF. (**b**) 4000-eV collisions with He; B/E linked scans recorded with the array detector.

The CVCID spectrum of BPDE-7-GSH is similar to that of BPDE-10-GSH. The interpretations of the CID spectra of the BPDE-GSH isomers is greatly aided by comparison with the CID spectra of LTC_4 recorded under identical instrumental conditions [26]. All ions assigned as peptide fragments are observed in the spectra of LTC_4. Furthermore, as can be seen from Table 2, the ions proposed to be formed by fragmentation of the BP-triol are common to the spectra of other BPDE-cysteinyl conjugates.

There have been comparatively few studies of the CID of conjugated BP metabolites. Gross and coworkers [22] have investigated the CID reactions BPDE-DNA adducts, while Zaia and Biemann [23] have investigated the fragmentation reactions of other BPDE-peptide adducts. In both of these studies positive-ion FAB was the method of ionization and kiloelectronvolt CID reactions of $[M + H]^+$ ions were investigated. In Gross's work on BPDE-DNA adducts, CID spectra of BPDE-10-Gua and BPDE-10-Ade were recorded. These were dominated by intense peaks at m/z 303 (A) corresponding to the BP-triol and at m/z

285 (A-H_2O), 257 (A-46), and 239 (A-64) resulting from losses of H_2O, CO, and a second H_2O from the triol portion of the molecule (Scheme II). Zaia and Biemann in their study also observed these fragment ions and also an ion at 267 (A-2H_2O). In both of these positive-ion studies $[M + H - 302]^+$ ions were observed. Branco et al. [24] investigated the positive-ion FAB, low energy CID of BPDE-DNA adducts. Their results were essentially similar to those of Gross and co-workers [22], indicating that the formation of ions at m/z 303, 285, 257, and 239 and corresponding to $[M + H - 302]^+$ are low energy processes. In our negative-ion CID spectra of the conjugated MP metabolites $[M - H - 302]^-$ ions (γ) were predominantly observed in the 4000-eV spectra although they were also present to a lesser extent in the 400-eV spectra. In spectra recorded at collision energies of 400 or 4000 eV there was no evidence of peaks at m/z 303, but the presence of fragment ions at m/z 285 and 257 is characteristic of BPDE-10 conjugates while peaks at m/z 267 and 239 were present in the spectra of BPDE-10 and BPDE-7 conjugates.

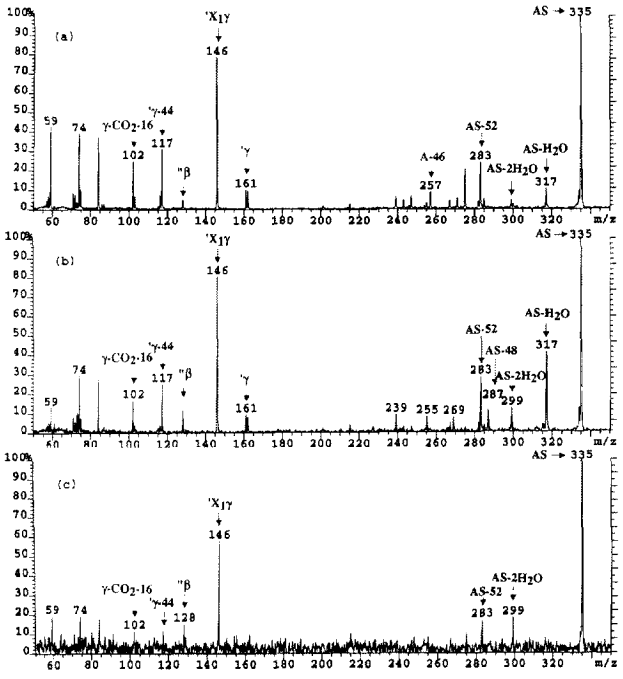

Figure 3. CID spectra of the $[M - H]^-$ ion of BPDE-NAcCys (m/z 464). 400-eV collisions with Xe; spectra recorded with the OATOF. (**a**) BPDE-10-NAcCys; (**b**) BPDE-7-NAcCys; (**c**) from the medium acidic fraction of germ-free rat urine.

Collision-Induced Dissociation of BPDE-10-CysGly, BPDE-10-NAcCys, BPDE-7-NAcCys, BPDE-10-Cys, and BPDE-7-Cys

CID spectra of the BPDE-CysGly, BPDE-NAcCys, and BPDE-Cys isomers are described in Table 2 and 400-eV CID spectra of BPDE-10-NAcCys and BPDE-7-NAcCys are shown in Figure 3 (see also Scheme III) Their interpretation is simplified by taking into account the CID spectra of the GSH conjugate and those of cysteinyl leukotrienes previously reported [21, 26]. The CID spectra of all BPDE-10 conjugates are very similar. The only significant differences result from fragmentation of the different peptide-conjugating groups. The BPDE-7 conjugates can readily be differentiated from the BPDE-10 conjugates. The BPDE-7 conjugates show characteristic enhanced intensity of fragment ions at m/z 317, 299, and 287, and the reduced intensity of the ions at 285 and 257 in their spectra.

The CVCID spectra of the BPDE-cysteinyl adducts have also been recorded, and are described in Table 2. The BPDE-NAcCys isomers can be differentiated by the presence of peaks at m/z 285 and 257 in the spectrum of the BPDE-10-NAcCys isomer but not that of BPDE-7-NAcCys isomer.

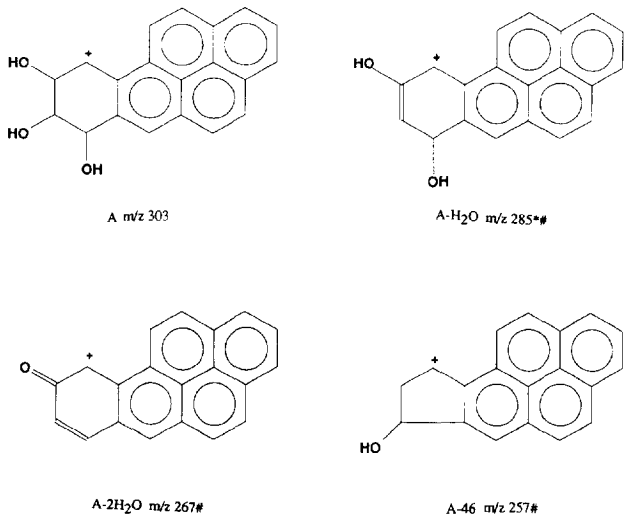

Scheme II. Fragment ions formed in the CID of $[M + H]^+$ BPDE-adducts [22, 24].

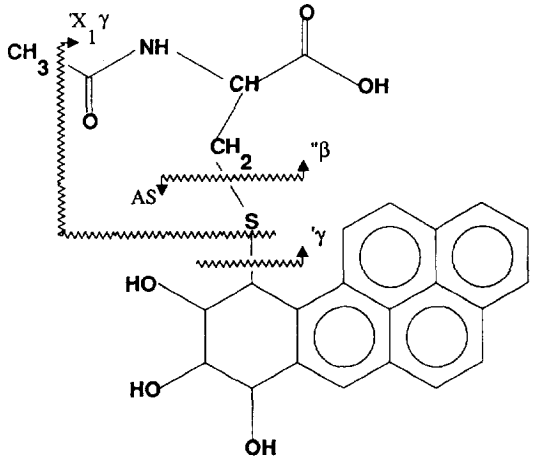

Scheme III. Fragmentation of BPDE-NAcCys. The peptide has been drawn conjugated to the BP-triol at position 10.

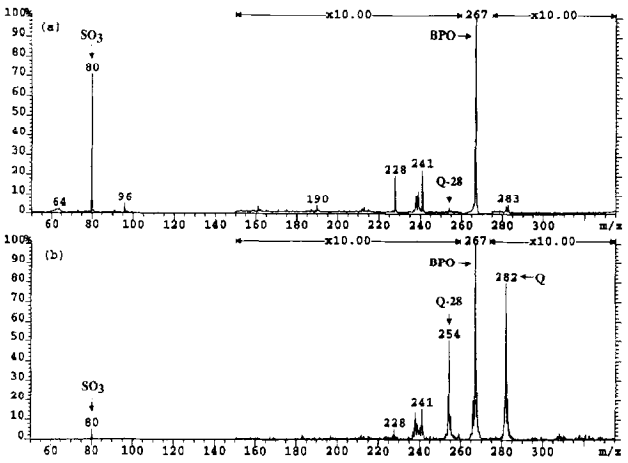

Figure 4. CID spectra of the $[M - H]^-$ ion of BP-9-SO_4 (m/z 347). (**a**) 400-eV collisions with Xe; spectrum recorded with the OATOF. (**b**) 4000-eV collisions with He; B/E linked scans recorded with the array detector.

Collision-Induced Dissociation of BP-9-Sulfate and BP-6-Sulfate

The CID spectra of the BP-9 sulfate is shown in Figure 4 (see Scheme IV). The fragmentation patterns observed at 400- and 4000-eV collision energies are similar. The only significant difference in the two spectra is in the intensity of fragment ions. In the 400-eV spectrum the dominant fragment ions are at m/z 267 (BPO) and 80 (SO_3), while in the 4000-eV spectrum the dominant fragment ions are at m/z 267 (BPO), 282 (Q), and 254 (Q–CO).

The CID spectra of BP-6-SO_4 (Figure 5) are very different from those of BP-9-SO_4. The 400-eV spectrum of BP-6-SO_4 is completely dominated by the SO_3 fragment ion at m/z 80. Other minor fragment ions are at 282 (Q) and 267 (BPO). In this spectrum the BPO and Q fragment ions have similar intensities, while in the corresponding spectrum of the BP-9-SO_4 isomer the BPO fragment was 50 times more intense.

The 4000-eV spectrum of BP-6-SO_4 (Figure 5b), like the 400-eV spectrum, shows an intense fragment at m/z 80. However, this spectrum is dominated by a fragment ion at m/z 282 (Q). The Q fragment in this spectrum is five times more intense than the BPO fragment. From the CID spectra recorded at both 4000 and 400 eV the two BP-SO_4 isomers can be easily differentiated.

The CVCID spectra of the two isomers are also different. The CVCID spectrum of BP-9-SO_4 is dominated by the BPO fragment as were the 400- and 4000-eV spectra of the isomer. The CVCID spectrum of BP-6-SO_4 shows an intense fragment ion at m/z 282, the characteristic fragmentation of BP-6-SO_4.

Collision-Induced Dissociation of BP-9-Glucuronide, BP-6-Glucuronide, and BP-3-Glucuronide

Neither the 4000- or 400-eV CID spectra allow the differentiation of the three BP-GlcA isomers. The 400-eV spectra are dominated by the BPO fragment (m/z 267) (Figure 6; Scheme V). At low mass, glucuronic acid fragment ions are observed. The 4000-eV spectra are similar to those recorded at 400 eV; however, the relative intensities of glucuronic acid fragments are reduced. The CVCID spectra of the three isomers are also indistinguishable, the only major fragment being at m/z 267.

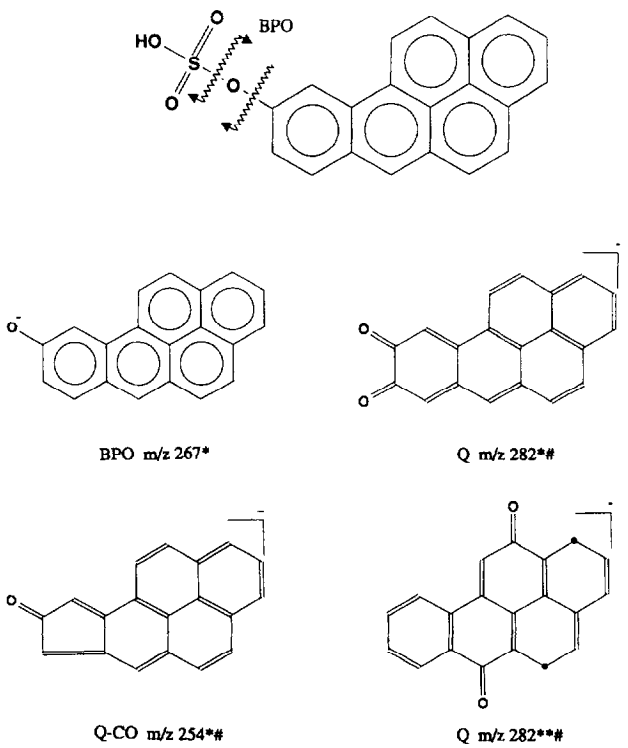

Scheme IV. Fragmentation of BP-SO_4. The sulfate has been drawn conjugated to the BP at position 9. Drawn for the 9-isomer (*), the 6-isomer (**), or the positional isomer (#).

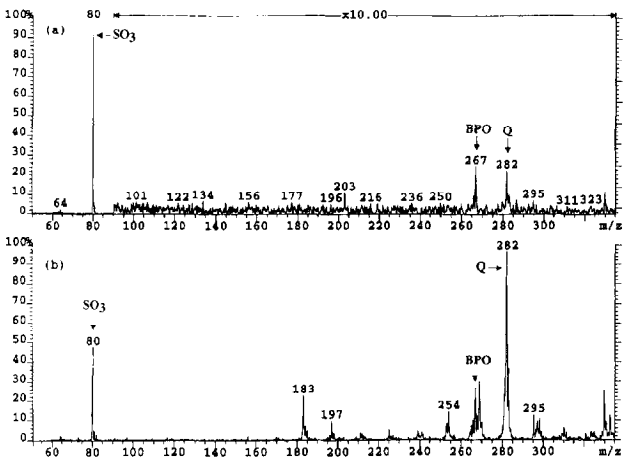

Figure 5. CID spectra of the $[M - H]^-$ ion of BP-6-SO_4 (m/z 347). (**a**) 400-eV collision with Xe; spectrum recorded with the OATOF. (**b**) 4000-eV collisions with He; B/E linked scans recorded with the array detector.

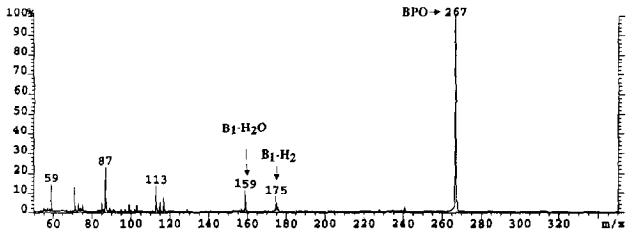

Figure 6. CID spectrum of the $[M - H]^-$ ion of BP-9-GlcA (m/z 443). 400-eV collisions with Xe; spectrum recorded with the OATOF.

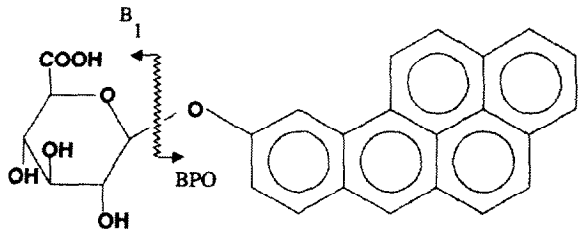

Scheme V. Fragmentation of BP-GlcA. The glucuronide has been drawn conjugated to the BP at position 9.

Gross and co-workers [22] also studied BP-6 adducts. They recorded CID spectra of the $[M + H]^+$ ions of BP-6-N7Gua, BP-6-C8Gua, BP-6-N^{2}dG, and BP-6-N7Ade and from them it was possible to differentiate between different isomers, for example, BP-N7Gua from BP-C8Gua, by differences in the ratio of two characteristic fragments at m/z 252 and 277. These ions correspond to BP radical cations and BP-CN radical cations. In the CID spectra of the $[M - H]^-$ ions of the BP-SO_4 and BP-GlcA isomers recorded in the present work BP radical anions were not observed, but BP–O fragment ions were observed in the spectra of all isomers.

Sensitivity of Negative-Ion Collision-Induced Dissociation for the Analysis of Conjugated BP Metabolites

A systematic study has not been made to determine the minimum amount of sample required to record a structurally informative CID spectrum. The aim of the present CID study was to investigate the fragmentation reactions of conjugated BP metabolites and thus spectra presented in Figures 1–6 were obtained from large quantities of sample (approximately 200 ng). However spectra containing the major fragment ions could be obtained from picomoles of infused sample.

Structure Determination of Conjugated BP Metabolites in the Urine of Germ-Free Rats by Using Micro-High-Performance Liquid Chromatography–Electrospray Mass Spectrometry–Collision-Induced Dissociation

Our previous study on BP metabolism in vivo by using ion exchange chromatography has shown that about 80% of the urinary metabolites of BP are in a conjugated form [7, 8]. Of these, 20% were sulfate conjugates eluting as strong acids and 40% were glucuronides and NAcCys conjugates eluting as acids of medium strength. By using capillary column HPLC-ES, mass spectra were recorded. By comparing the mass spectra of each component in each chromatographic fraction, collected from urine before and after BP administration, BP conjugates were identified in the complex mixture of endogenous compounds. In ongoing work, micro-HPLC-ES with CID is used to provide structural information concerning the various urinary conjugated BP metabolites.

As an example of this application of the methodology to the in vivo situation, the fraction from germ-free rat urine-containing acids of medium strength gave an intense ion at m/z 464 after but not prior to the administration of BP. The 400-eV CID spectrum of this ion was recorded and is described in Table 2 and shown in Figure 3c. The compound was identified as a BPDE-NAcCys isomer. A group of low mass peaks (m/z 59, 74, 102, 117, 128, 146, and 162) were observed which are characteristic of the NAcCys conjugating group. The most intense fragment is at m/z 335, which is characteristic of the tetrahydro-trihydroxy-sulfur modified BP ring (AS). However, the precursor ion does not appear to correspond to BPDE-10-NAcCys or BPDE-7-NAcCys as its fragmentation pattern, although similar to those of the isomers studied, is not identical. The most pronounced difference between the spectra is the greatly reduced intensity of the fragment ion at 317 in the CID spectrum of the metabolite in rat urine. Analysis of further reference compounds will be required to determine the position of conjugation.

Collision Energy Effects on Collision-Induced Dissociation Reactions

As mentioned above, the CID spectra recorded as B/E linked scans at a collision energy of 4000 eV showed differences from those recorded on the OATOF at collision energies of 400 eV. The major differences between the 400- and 4000-eV CID spectra of the conjugated BPDEs concerned the intensity of the low mass peptide fragment ions; otherwise the spectra recorded at the two collision energies are very similar. A comparable situation pertains to the CID of the isomers of BP-GlcA and BP-SO_4, where the intensity of the low mass fragment ions is accentuated in the 400-eV CID spectra.

CID reactions are often discussed in terms of center of mass collision energies (E_{cm}) and laboratory frame of reference collision energies (E_{lab}). E_{cm} values are calculated by using the equation

$$E_{cm} = E_{lab}[m_{cg}/(m_p + m_{cg})] \quad (1)$$

Table 3. Center of mass collision energies calculated for the CID of BP metabolite conjugates

BP-Metabolite	4-keV Collision with HE	400-eV Collision with Xe	300-eV Collision with N_2
BPDE-GSH	26	71	13
BPDE-CysGly	33	86	17
BPDE-NAcCys	34	89	17
BPDE-Cys	38	95	19
BP-sulfate	46	110	22
BP-glucuronide	36	92	18

where E_{lab} is the initial kinetic energy of the projectile ion, m_p is the mass of the projectile ion, and m_{cg} is the mass of the collision gas.

Values of E_{cm} give the maximum theoretical amount of the projectile ions translational energy that can be converted into internal energy as the result of the collision, and those calculated for the collision reactions studied are given in Table 3. Very often CID spectra recorded at quite different laboratory frame collision energies but with center of mass collision energies above a certain threshold give similar spectra. This has been shown to be true of peptides [27], fatty acids [28], and leukotrienes [21, 26] and also holds for conjugated BPDE and BPs.

Conclusion

Micro-column HPLC interfaced to a hybrid magnetic sector tandem mass spectrometer with electrospray ionization is a promising method for the study of intact conjugated BP metabolites. With a focal plane array detector, detection limits were at the femtomole level. This will allow us to detect labile conjugated BP metabolites in biological samples at trace levels. Structure elucidation of individual BP conjugates was achieved by CID. The CID spectra can be used not only to determine the type of conjugation of BP metabolites, but also in some cases the position of conjugation.

Acknowledgments

This work was supported by the Swedish Cancer Society, Swedish Medical Research Council (grants 03X-6805, 13X-219, 16X-6852, and 03Y-10826), Cancerföreningen (Stockholm), and the Karolinska Institute. The authors wish to thank R. Reimendal and N. Hammar of the Department of Medical Biochemistry and Biophysics, Karolinska Institute, T. Midtvedt of the Department of Medical Microbial Ecology, Karolinska Institute, B. Egestad of Neurosearch A/S Denmark, and M. Porter, R. Vickers, K. Howes, A. Woolfitt, A. Brown, P. Bamforth, J. Watkins, and A. Casen of Micromass for expert technical assistance. We are also grateful to C. L. Griffiths for production of tables.

References

1. *IARC Monographs on the Evaluation of Carcinogenic Risks of Chemicals to Man, International Agency for Research on Cancer*; IARC, Lyon, France, 1973; p. 3.
2. Conney, A. H.; Chang, R. L.; Jerina, D. M.; Wei, S.-J. C. *Drug Metabolism Rev.* **1994**, *261*, 125–163.
3. Jernström, B.; Gräslund, A. *Biophys. Chem.* **1994**, *49*, 185–199.
4. Depierre, J.; Ernster, L. *Biochim. Biophys. Acta* **1978**, *473*, 149–158.
5. Chasseaud, L. F. In *Glutathione: Metabolism and Function*; Arias, I. M.; Jakoby, W. B., Eds.; Raven: New York, 1976; pp 77–114.
6. Rafter, J.; Bakke, J.; Larsen, G.; Gustafsson, B.; Gustafsson, J.-Å. *Rev. Biochem. Toxicol.* **1983**, *5*, 387–408.
7. Egestad, B.; Pettersson, P.; Sjövall, J.; Rafter, J.; Hyvönen, K.; Gustafsson, J.-Å. *Biomed. Chromatogr.* **1987**, *2*, 120–134.
8. Yang, Y.; Egestad, B.; Rafter, J. *Proceeding of the VIIIth International Symposium on Microsomes and Drug Oxidations*; Karolinska Institute, Stockholm, Sweden, June 1990; p 397.
9. Grover, P. L. *Xenobiotica* **1986**, *16*, 915–931.
10. Cooper, C. S.; Grover, P. L.; Sims, P. *Prog. Drug Metabolism* **1983**, *7*, 295–395.
11. Yang, Y.; Sjövall, J.; Rafter, J.; Gustafsson, J.-Å. *Carcinogenesis* **1994**, *15*, 681–687.
12. Yang, Y.; Egestad, B.; Jernström, B.; Sjövall, J.; Gustafsson, J.Å.; Rafter, J. *Rapid Commun. Mass Spectrom.* **1991**, *5*, 499–502.
13. Teffera, Y.; Baird, W. M.; Smith, D. L. *J. Chromatog.* **1992**, *577*, 69–76.
14. Bieri, R. H.; Greaves, J. *Biomed. Environ. Mass Spectrom.* **1987**, *14*, 555–561.
15. Fenn, J. B.; Mann, M.; Meng, C. K.; Wong, S. K.; Whitehouse, C. *Mass Spectrom. Rev.* **1990**, *9*, 37–70.
16. Yang, Y.; Griffiths, W. J.; Lindgren, J.Å.; Sjövall, J. *Rapid Commun. Mass Spectrom.* **1995**, *9*, 289–299.
17. Bateman, R. H.; Green, M. R.; Scott, G.; Clayton, E. *Rapid Commun. Mass Spectrom.* **1995**, *9*, 1227–1233.
18. Griffiths, W. J.; Hjertman, M.; Lundsjö, A.; Wejde, J.; Sjövall, J.; Larsson, O. *Rapid Commun. Mass Spectrom.* **1996**, *10*, 663–675.
19. Alborn, H.; Stenhagen, G. *J. Chromatogr.* **1985**, *323*, 47–66.
20. Roepstorff, P.; Fohlman, J. *Biol. Mass Spectrom.* **1984**, *11*, 601.
21. Griffiths, W. J.; Yang, Y.; Sjövall, J.; Lindgren, J. Å. *Rapid Commun. Mass Spectrom.* **1996**, *10*, 1504–1070.
22. RamaKrishna, N. V. S.; Gao, F.; Padmavathi, N. S.; Cavalieri, E. L.; Rogan, E. G.; Cerny, R. L.; Gross, M. L. *Chem. Res. Toxicol.* **1992**, *5*, 293–302.
23. Zaia, J.; Biemann, K. *J. Am. Soc. Mass Spectrom.* **1994**, *5*, 649–654.
24. Branco, S.; Chiarelli, M. P.; Lay, J. O., Jr.; Beland, F. A. *J. Am. Soc. Mass Spectrom.* **1995**, *6*, 248–256.
25. Deterding, L. J.; Srinivas, P.; Mahmood, N. A.; Burka, L. T.; Tomer, K.; *Anal. Chem.* **1989**, *183*, 94.
26. Griffiths, W. J.; Yang, Y.; Lindgren, J. Å.; Sjövall, J. *Proceedings of the 44th ASMS Conference on Mass Spectroscopy and Allied Topics*; Portland, Oregon, May 1996.
27. Lindh, I.; Griffiths, W. J.; Bermgan, T.; Sjövall, J. *Proceedings of the 44th ASMS Conference on Mass Spectroscopy and Allied Topics*; Portland, Oregon, May 1996.
28. Griffiths, W. J.; Yang, Y.; Lindgren, J. Å.; Sjövall, J. *Rapid Commun. Mass Spectrom.* **1996**, *10*, 21–28.